

New Measurements of the Deuteron to Proton F_2 Structure Function Ratio

D. Biswas,¹ F. Gonzalez,² W. Henry,³ A. Karki,⁴ C. Morean,⁵ A. Nadeeshani,¹ A. Sun,⁶ D. Abrams,⁷ Z. Ahmed,⁸ B. Aljawrneh,⁹ S. Alsalmi,^{10,11} R. Ambrose,⁸ W. Armstrong,¹² A. Asaturyan,³ K. Assumin-Gyimah,⁴ C. Ayerbe Gayoso,^{13,4} A. Bandari,¹³ S. Basnet,⁸ V. Berdnikov,¹⁴ H. Bhatt,⁴ D. Bhetuwal,⁴ W. U. Boeglin,¹⁵ P. Bosted,¹³ E. Brash,¹⁶ M. H. S. Bukhari,¹⁷ H. Chen,⁷ J. P. Chen,³ M. Chen,⁷ M. E. Christy,^{1,3} S. Covrig,³ K. Craycraft,⁵ S. Danagoulian,⁹ D. Day,⁷ M. Diefenthaler,³ M. Dlamini,¹⁸ J. Dunne,⁴ B. Duran,¹² D. Dutta,⁴ R. Ent,³ R. Evans,⁸ H. Fenker,³ N. Fomin,⁵ E. Fuchey,¹⁹ D. Gaskell,³ T. N. Gautam,¹ F. A. Gonzalez,² J. O. Hansen,³ F. Hauenstein,^{20,3} A. V. Hernandez,¹⁴ T. Horn,¹⁴ G. M. Huber,⁸ M. K. Jones,³ S. Joosten,²¹ M. L. Kabir,⁴ C. Keppel,³ A. Khanal,¹⁵ P. M. King,¹⁸ E. Kinney,²² M. Kohl,¹ N. Lashley-Colthirst,¹ S. Li,²³ W. B. Li,¹³ A. H. Liyanage,¹ D. Mack,³ S. Malace,³ P. Markowitz,¹⁵ J. Matter,⁷ D. Meekins,³ R. Michaels,³ A. Mkrtchyan,²⁴ H. Mkrtchyan,²⁴ Z. Moore,²⁵ S.J. Nazeer,¹ S. Nanda,⁴ G. Niculescu,²⁵ I. Niculescu,²⁵ D. Nguyen,⁷ Nuruzzaman,²⁶ B. Pandey,^{1,27} S. Park,² E. Pooser,³ A. J. R. Puckett,¹⁹ M. Rehfuss,¹² J. Reinhold,¹⁵ B. Sawatzky,³ G. R. Smith,³ H. Szumila-Vance,³ A. S. Tadealli,²⁶ V. Tadevosyan,²⁴ R. Trotta,¹⁴ S. A. Wood,³ C. Yero,^{15,14} and J. Zhang²

(for the Hall C Collaboration)

¹Hampton University, Hampton, Virginia 23669, USA

²Stony Brook University, Stony Brook, New York 11794, USA

³Thomas Jefferson National Accelerator Facility, Newport News, Virginia 23606, USA

⁴Mississippi State University, Mississippi State, Mississippi 39762, USA

⁵University of Tennessee, Knoxville, Tennessee 37996, USA

⁶Carnegie Mellon University, Pittsburgh, Pennsylvania 15213, USA

⁷University of Virginia, Charlottesville, Virginia 22903, USA

⁸University of Regina, Regina, Saskatchewan S4S 0A2, Canada

⁹North Carolina A & T State University, Greensboro, North Carolina 27411, USA

¹⁰Kent State University, Kent, Ohio 44240, USA

¹¹King Saud University, Riyadh 11451, Saudi Arabia

¹²Temple University, Philadelphia, Pennsylvania 19122, USA

¹³The College of William & Mary, Williamsburg, Virginia 23185, USA

¹⁴Catholic University of America, Washington, DC 20064, USA

¹⁵Florida International University, University Park, Florida 33199, USA

¹⁶Christopher Newport University, Newport News, Virginia 23606, USA

¹⁷Jazan University, Jazan 45142, Saudi Arabia

¹⁸Ohio University, Athens, Ohio 45701, USA

¹⁹University of Connecticut, Storrs, Connecticut 06269, USA

²⁰Old Dominion University, Norfolk, Virginia 23529, USA

²¹Argonne National Laboratory, Lemont, Illinois 60439, USA

²²University of Colorado Boulder, Boulder, Colorado 80309, USA

²³University of New Hampshire, Durham, New Hampshire 03824, USA

²⁴A.I. Alikhanyan National Science Laboratory

(Yerevan Physics Institute), Yerevan 0036, Armenia

²⁵James Madison University, Harrisonburg, Virginia 22807, USA

²⁶Rutgers University, New Brunswick, New Jersey 08854, USA

²⁷Virginia Military Institute, Lexington Virginia, 24450 USA

(Dated: August 28, 2024)

Nucleon structure functions, as measured in lepton-nucleon scattering, have historically provided a critical observable in the study of partonic dynamics within the nucleon. However, at very large parton momenta it is both experimentally and theoretically challenging to extract parton distributions due to the probable onset of non-perturbative contributions and the unavailability of high precision data at critical kinematics. Extraction of the neutron structure and the d-quark distribution have been further challenging due to the necessity of applying nuclear corrections when utilizing scattering data from a deuteron target to extract free neutron structure. However, a program of experiments has been carried out recently at the energy-upgraded Jefferson Lab electron accelerator aimed at significantly reducing the nuclear correction uncertainties on the d-quark distribution function at large partonic momentum. This allows leveraging the vast body of deuterium data covering a large kinematic range to be utilized for d-quark parton distribution function extraction. In this paper we present new data from experiment E12-10-002 carried out in Jefferson Lab Experimental Hall C on the deuteron to proton cross-section ratio at large Bjorken- x . These results significantly improve the precision of existing data, and provide a first look at the expected impact on quark distributions extracted from global parton distribution function fits.

Measurements of the nucleon F_2 structure function in inelastic lepton-nucleon scattering and the kinematic evolution of F_2 occupy a prominent place in the historical development and testing of the theory of the strong interaction, Quantum Chromodynamics (QCD) [1–3]. Such measurements have provided critical data in perturbative QCD (pQCD) fits used to extract quark and gluon distributions and in testing the universality of the pQCD evolution equations of these parton distribution functions (PDFs) [4–6]. While tremendous progress has been made in this endeavor over the last few decades, much is still left to be fully explored. One such example is the longitudinal momentum distribution of the down quarks when the nucleon’s momentum is predominantly carried by a single valence quark, or as $x \rightarrow 1$. Here x is the Bjorken “scaling” variable which can be interpreted as the fractional momentum of the nucleon carried by the struck quark. While there exists a number of effective theory predictions [5–9] for the ratio of the down to up quark distributions (d/u) at large x , additional experimental data are required to adequately test these. The last few years have seen the completion of three complementary experiments performed at Jefferson Lab utilizing the energy-upgraded CEBAF accelerator and aimed at extracting the neutron to proton F_2 ratio and providing access to d/u at large x . The first of these was the MARATHON [13] experiment in Hall A, which measured ratios of the inclusive structure function F_2 from the $A=3$ mirror nuclei ${}^3\text{He}$ and ${}^3\text{H}$, as well as from the deuteron and proton. The second experiment was the BONuS12 [14] experiment in Hall B, which is a follow-up to the BONuS [15–17] experiment, but leveraging the doubling of the beam energy to 12 GeV to access larger x without entering the region of the nucleon resonances. Jefferson Lab (JLab) experiment E12-10-002 (this work) measured $H(e, e')$ and $D(e, e')$ inclusive cross-sections with the aim of extracting the hydrogen and deuterium F_2 structure functions at large x and intermediate four-momentum transfer, Q^2 . The new high-precision data from this work, especially when coupled with new nuclear correction data from BONuS12 and MARATHON, will provide new insight into the up and down quark distributions within the nucleon.

The dataset was acquired in February–March of 2018 in Hall C. The experiment used the standard Hall C equipment: the High Momentum Spectrometer (HMS), the SuperHMS (SHMS), and liquid cryogenic hydrogen and deuterium targets. The electron beam energy was 10.602 GeV and the current varied between 30 and 65 μA . The experiment served as one of the commissioning experiments for the new or upgraded Hall C equipment associated with the JLab 12 GeV energy upgrade. The data were acquired in “scans” at a fixed spectrometer angle by varying the central momentum setting and alternating between the 10 cm long hydrogen and deuterium targets. The results presented here stem from five different SHMS scans at (nominal) scattering angles of 21, 25, 29, 33, and 39 degrees. The central momentum varied

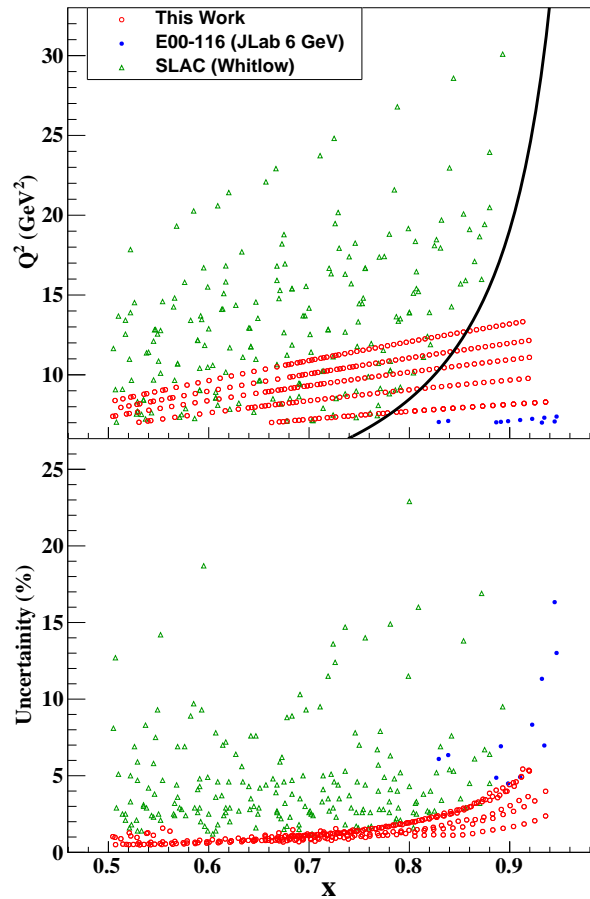


FIG. 1. The top panel shows the kinematic coverage of this work (red circles), compared with the Whitlow reanalysis [10, 11] existing SLAC data (green triangles). The solid blue circles are from JLab’s 6 GeV experiment, E00-116 [12]. Only data where $x > 0.5$ and $Q^2 > 6$ are shown. The solid curve indicates $W^2 = 3 \text{ GeV}^2$, where W is the invariant mass of the produced hadronic system. The statistical uncertainty of the deuteron to hydrogen cross-section ratio from these experiments are shown in the bottom panel.

between 1.3 and 5.1 GeV/c. Additional scans were taken with the HMS at 21 and 59 degrees. The 21 degree data were used as a cross-check between the well understood HMS and the newly constructed SHMS. The 59 degree data are still being analyzed and are not presented here. The kinematic coverage of this work, in Q^2 and x coordinates, is shown in Figure 1, also displayed are the world data from SLAC (green triangles) and 6 GeV JLab (blue solid circles). Prior to this work, the invariant mass region of $W^2 < 3 \text{ GeV}^2$, (i.e. to the right of the solid curve), is poorly populated above a Q^2 of about 6 GeV^2 . The statistical uncertainties of this work, shown in the top panel of Fig.1, are a vast improvement over existing data.

The SHMS is a new spectrometer installed in Hall C to take advantage of the energy upgrade of the CEBAF ac-

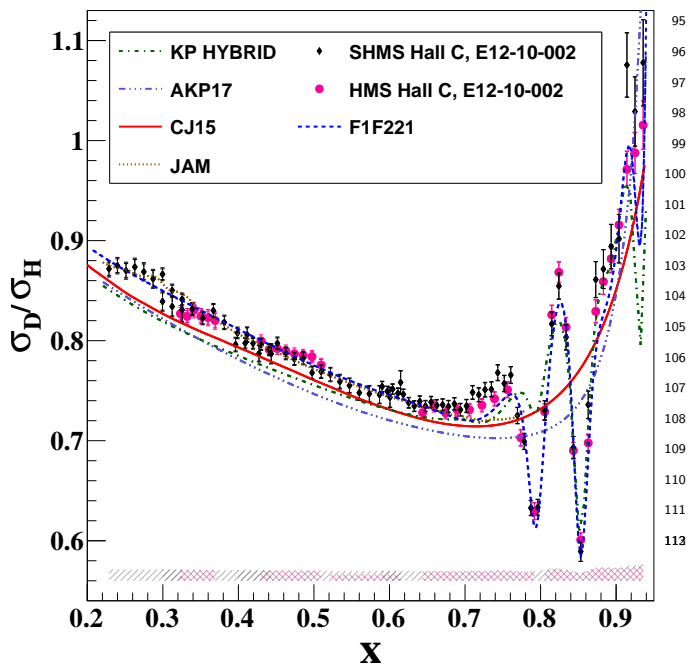


FIG. 2. The σ_D/σ_H ratio as a function of x for a spectrom-114
eter angle of 21 deg (Q^2 range from 3.39 to 8.25 GeV²). To115
first order, the cross section ratio is equal to the F_2 structure116
function ratio. The error bars include uncorrelated system-117
atic and statistical errors. The error bands include correlated118
systematic errors and an overall normalization uncertainty of119
1.1%(see Table I). F1F221 (blue dashed line) is the model120
used in this analysis, the other curves are from different PDF121
fits (see text). Good agreement is observed between the well-122
understood HMS and newly constructed SHMS spectrome-123
ters.124

76 celerator to 12 GeV. [18–20]. Its magnetic layout consists,126
77 of a horizontal bender, three quadrupoles, and a dipole,127
78 ($HQQQD$). The maximum momentum is 11.0 GeV/c,128
79 the typical momentum acceptance is -10% to 22% about,129
80 the central momentum, and the solid angle is ~ 4.0 msr.130
81 The standard detector package includes a gas Cherenkov131
82 detector (filled with 1 atm of CO₂) and an electromag-132
83 netic calorimeter for particle identification (PID), two,133
84 wire drift chambers for tracking and event reconstruc-134
85 tion, and four hodoscope planes used in the event trigger.135
86 An additional heavy gas Cherenkov and aerogel detector,136
87 were present in the detector package but not used in this,137
88 analysis as they are primarily used for hadron identifica-138
89 tion.139

90 In the one-photon exchange approximation the differ-140
91 ential cross-section for inclusive electron scattering can,141
92 be written as:142

$$\frac{d^2\sigma}{d\Omega dE'} = \sigma_{\text{Mott}} \frac{2MxF_2}{Q^2\varepsilon} \left(\frac{1 + \varepsilon R}{1 + R} \right) \quad (1)$$

93 Where σ_{Mott} is the Mott cross-section, M is the nucleon,147
94 mass, Q^2 is the negative of the four-momentum transfer148

squared, R is the ratio of the longitudinal to transverse
photoabsorption cross-sections ($R = \sigma_L/\sigma_T$) and ε is
the virtual photon polarization. The aim of this work
is to obtain the F_2^D/F_2^H structure function ratio, as it
presents several advantages theoretically as well as exper-
imentally. By reporting a quantity involving deuterium
rather than the (“free”) neutron, we avoid choosing a
particular prescription for treating nuclear effects, allow-
ing theory groups active in this field to extract F_2^D using
their own nuclear corrections. Furthermore, the σ_L/σ_T
ratio is largely the same for hydrogen and deuterium [21],
thus, to first order, the F_2^D/F_2^H ratio is the same as the
cross-section ratio. The experimental advantage of report-
ing a cross section ratio is that several corrections
to the yield cancel (e.g. detector efficiencies) and mul-
tiple systematic errors are reduced such as the effective
target length, deadtime corrections and spectrometer ac-
ceptance.

Experimentally, the cross-section is obtained using the
Monte Carlo ratio method [22]

$$\left(\frac{d^2\sigma}{d\Omega dE'} \right)_{\text{Exp}} = \frac{Y_{\text{Data}}}{Y_{\text{MC}}} \left(\frac{d^2\sigma}{d\Omega dE'} \right)_{\text{Model}} \quad (2)$$

where Y_{Data} is the efficiency and background corrected
charge normalized electron yield, Y_{MC} is the Monte Carlo
yield obtained using a model cross-section that is radi-
ated using the Mo and Tsai formalism [23, 24], and
 $(d^2\sigma/d\Omega dE')_{\text{Model}}$ is the same model cross-section eval-
uated at the Born level. The yields were binned in W^2 ,
and then converted to x . Electrons were selected by
applying cuts to the gas Cherenkov and the energy de-
posited in the calorimeter normalized by the momentum
of the track.

Corrections to Y_{Data} , along with their relative magni-
tudes in the inelastic region ($W^2 > 3$ GeV²), include
contributions from pion contamination (0.829-0.999), dead-
time (1.002-1.668), target density (1.008-1.029), tracking
efficiency (1.001-1.065), trigger efficiency (1.001-1.002),
and backgrounds from the target cell walls (0.888-0.982).
Pions that pass the electron PID cuts were removed using
a parameterization of the pion contamination as a
function of the scattered electron energy, E' [25]. The
computer deadtime was found by comparing the number
of triggers recorded in scalars to the number found in
the datastream. The electronic deadtime, due to events
being lost at the trigger logic level, was measured by in-
jecting a pulser of known frequency at the start of the
trigger logic chain. These pulser events, identifiable via
TDC information, were compared with the number of
events recorded in the scalars. Tracking efficiency was
calculated by taking the ratio of events with detected
tracks to the number of events that passed PID, fidu-
cial and timing cuts. The trigger for this experiment re-
quired signals in 3 of the 4 hodoscope layers and a signal
in either the gas Cherenkov or calorimeter. The trig-
ger efficiency was $> 99\%$ and determined by calculating
the efficiency of the individual hodoscope planes. Back-
grounds from the aluminum cell walls were subtracted

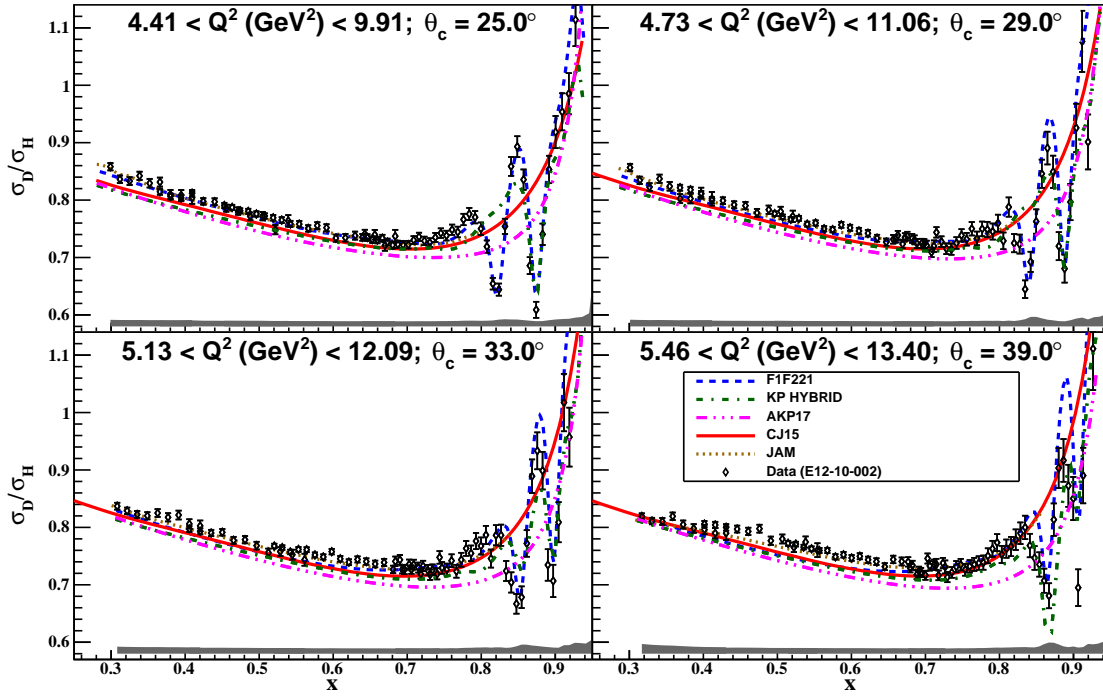


FIG. 3. The cross section ratio, σ_D/σ_H , as a function of x for SHMS spectrometer angles of 25, 29, 33, and 39 deg. To first order, the cross section ratio is equal to the F_2 structure function ratio. The Q^2 range of each setting is indicated in each panel.

149 from the cryogenic targets by utilizing “dummy” data
 150 taken on two aluminum targets placed at the same loca-
 151 tion as the cryogenic entrance and exit windows. A
 152 target density correction was applied to account for a lo-
 153 cal change in density due to heating from the electron
 154 beam. A series of dedicated measurements at various
 155 currents up to $80 \mu\text{A}$ were performed and the charge
 156 normalized yields were plotted vs beam current. The
 157 density reduction for the hydrogen (deuterium) target
 158 was $2.55 \pm 0.74 \frac{\%}{100 \mu\text{A}}$ ($3.09 \pm 0.84 \frac{\%}{100 \mu\text{A}}$). For further
 159 details of the analysis see [25–30].

160 Electrons produced by charge symmetric backgrounds,
 161 mainly from neutral pion production (e.g. $\pi^0 \rightarrow \gamma\gamma^* \rightarrow$
 162 $\gamma e^+ e^-$), in which the photon decays into a positron and
 163 an electron were included in the Monte Carlo yield. This
 164 background was measured by reversing the spectrome-
 165 ters’ magnet polarity to measure the positron yield for
 166 both hydrogen and deuterium targets. The background
 167 was parameterized with a two parameter fit as a func-
 168 tion of E' . Due to beam time constraints, positron data
 169 was acquired for only three of the five angular settings.
 170 To circumvent this limitation, the positron yield was pa-
 171 rameterized as described in [31]. The parameterization
 172 was then used to extrapolate the positron yield to the
 173 kinematic settings where measurements were not avail-
 174 able. For $x > 0.6$, the background contribution to the
 175 measured cross-section was less than 1% and rose to 30%
 176 with decreasing x at the 39 degree angle setting. Ad-
 177 ditionally, the measured positron yield per nucleon was

Error	Pt. to Pt (%)	Correlated (%)
Statistical	0.5 – 5.4(2.9)	
Charge	0.1 – 0.6	
Target Density	0.0 – 0.2	1.1
Livetime		0.0 – 1.0
Model Dependence		0.0 – 2.6(1.2)
Charge Sym. Background		0.0 – 1.4
Acceptance		0.0 – 0.6(0.3)
Kinematic		0.0 – 0.4
Radiative Corrections		0.5 – 0.7(0.6)
Pion Contamination		0.1 – 0.3
Cherenkov Efficiency		0.1
Total	0.6 – 5.4(2.9)	1.2 – 2.9(2.1)

TABLE I. The error budget for the cross-section ratio σ_D/σ_H . The error after a cut of $W^2 > 3 \text{ GeV}^2$ is shown in parenthesis, which is a typical cut applied to eliminate the resonance region while performing PDF fits.

identical for both targets, canceling out in the ratio.

The uncertainties in the deuterium to hydrogen cross-section ratio σ_D/σ_H , shown in Table I, are divided into two categories, uncorrelated point-to-point and correlated. An overall normalization uncertainty of 1.1% due to uncertainty in the target density is included in the correlated error. The target density error includes uncertainties from the target temperature and pressure, mea-

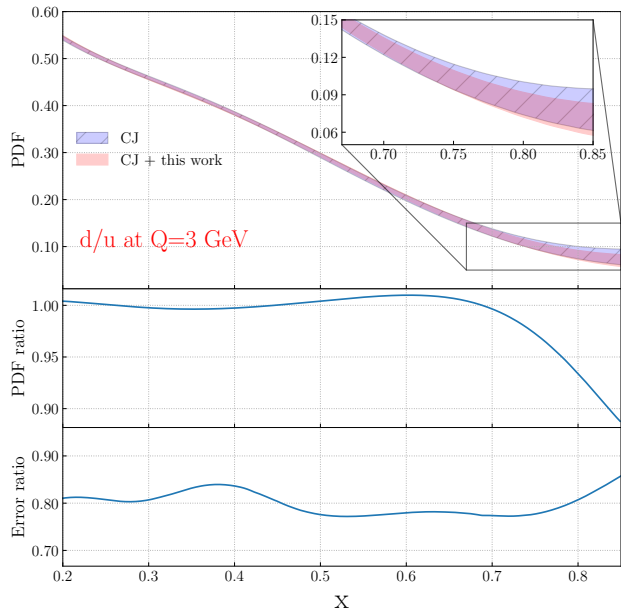


FIG. 4. Top: The CJ15 d/u PDF fit before (red) and after (blue) the inclusion of this work. Middle: The reduction in the d/u PDF relative uncertainty. The inclusion of the data from this work results in a roughly 20% reduction in the uncertainty. Bottom: The relative change in the d/u PDF central value, the shift at $x > 0.7$ is due to the previous lack of deuterium data at high- x . While a typical cut of $W^2 > 3.0$ GeV² is used to eliminate the resonance region in the CJ15 framework, a cut of $W^2 > 3.5$ GeV² was applied to the new dataset.

dashed violet line), KP Hybrid[8] (dot-dashed line) and JAM [33, 34] (dotted brown line). The model used to extract the cross-section is F1F221 (dashed blue line) which is an improved fit to world data [35]. None of the models shown includes the data from this analysis.

The impact of the data from this work was evaluated with the CJ15 QCD analysis [9] framework, which deploys state-of-the-art deuteron nuclear corrections and leverages recent result. A fitted normalization factor of -2.1% was determined in order for the data set to agree with the CJ model [36], slightly larger than the total x dependent correlated error of 1.3% - 2.1% shown in Table I. Furthermore, this experiment ran in parallel with E12-10-007 (a measurement of the EMC effect) which observed a 2.0% normalization difference with previous EMC measurements[37], the direction of this normalization difference is consistent with that found in the CJ15 study. The fitted PDFs with and without this experiment were compared at the central value as well as the size of uncertainties. For consistency, the error band for each fit was calculated at 90% confidence level [38]. Fig. 4 depicts the d/u ratio, a fundamental quantity and testing ground for multiple (p)QCD predictions regarding nucleon structure. The fitted d/u PDF before and after inclusion of this data is shown, where the significant reduction in the uncertainties demonstrates the importance of high precision data in PDF extractions. Not only did the inclusion of this work reduce the relative error by approximately 20% across the entire x range, but it also shifted the d/u central value at large- x by as much as 10%. Furthermore, this data provides additional constraints on the parameters used in higher twist corrections, the individual d and u quark distributions, and the target mass corrections used in these fits.

It should be noted that, on average, the deuterium to hydrogen cross section ratio from this work and MARATHON[39] differ by as much as 4.3% or 2σ where the datasets overlap in the x range of $0.2 - 0.3$, with this work being above the MARATHON result. However, in a recent global QCD analysis[40] a normalization factor of $+1.9\%$ was required in order for the MARATHON d/p data to agree with existing data. If this normalization is applied, together with the normalization factor found from the above CJ15 study the two datasets agree within 0.3% . All the aforementioned data agree with the previously available SLAC data, which have large uncertainties [10].

In summary, high-precision inclusive measurements on hydrogen and deuterium were performed for Q^2 from 3.4 to 13.4 GeV² and x from 0.3 to 0.93 . This data, especially when combined with the MARATHON and BoNUS results, has a significant impact on PDF fitting efforts. It can be used, moreover, for quark-hadron duality studies, spin-flavor symmetry breaking, and constraints on nuclear corrections. Additionally, knowledge of PDF fits at large- x is essential for determining high energy cross-sections at the future EIC, where structure function information at large x feeds down through perturbative

186 sured length, thermal contraction, the equation of state
 187 used to calculate the density, and the target boiling cor-
 188 rection. Additional point-to-point errors for target den-
 189 sity are included to account for runs where the boiling
 190 correction was far from the average due to higher or lower
 191 beam currents. A Monte Carlo cross-section model de-
 192 pendence error was assessed by repeating the analysis
 193 with various models and comparing the resulting cross-
 194 sections. The most significant effects were observed at
 195 higher x values, where the resonance region causes rapid
 196 changes in the cross-section. Binning in W^2 was found to
 197 reduce this uncertainty. Errors from the radiative correc-
 198 tions include a contribution from both the model and the
 199 method. The model dependence was determined by scal-
 200 ing the various quasi-elastic contributions to the model.
 201 The error associated with the method (0.5%) was taken
 202 from [32]. A kinematic uncertainty was determined with
 203 Monte Carlo by individually varying the beam energy
 204 and central momentum of the spectrometer by $\pm 0.1\%$
 205 and also by varying the spectrometer angle by ± 0.25 mrad.
 206 The results of this analysis are summarized in Fig. 2
 207 and Fig. 3. The σ_D/σ_H ratio is shown as a function of
 208 x for each of the SHMS spectrometer angles. The curves
 209 shown are predictions for F_2^D/F_2^H obtained using four
 210 available models evaluated at the same kinematics as the
 211 data: CJ15 [9] (solid red line), AKP17 [7] (dot-dot-dot-

270 Q^2 evolution to lower x and higher values of Q^2 , and²⁷⁵
 271 for higher precision neutrino oscillation Monte Carlos for²⁷⁶
 272 DUNE [41].²⁷⁷

273 This material is based upon work supported by the²⁷⁸
 274 U.S. Department of Energy, Office of Science, Office of

Nuclear Physics under contracts DE-AC05-06OR23177,
 DE-AC02-05CH11231, DE-SC0013615, and DE-FE02-
 96ER40950, and by the National Science Foundation
 (NSF) Grant No. 1913257.

-
- 279 [1] R. E. Taylor, *Rev. Mod. Phys.* **63**, 573 (1991). 319
 280 [2] H. W. Kendall, *Rev. Mod. Phys.* **63**, 597 (1991). 320
 281 [3] J. I. Friedman, *Rev. Mod. Phys.* **63**, 615 (1991). 321
 282 [4] A. Accardi *et al.*, *Phys. Rev. D* **81**, 034016 (2010). 322
 283 [5] S. I. Alekhin, *Phys. Rev. D* **63**, 094022 (2001). 323
 284 [6] S. I. Alekhin, *Phys. Rev. D* **68**, 014002 (2003). 324
 285 [7] S. I. Alekhin, S. A. Kulagin, and R. Petti, *Phys. Rev. D* **96**, 054005 (2017), arXiv:1704.00204 [nucl-th]. 325
 286 [8] S. A. Kulagin, *Phys. Part. Nucl.* **50**, 506 (2019), arXiv:1812.11738 [nucl-th]. 326
 287 [9] A. Accardi, L. T. Brady, W. Melnitchouk, J. F. Owens, and N. Sato, *Phys. Rev. D* **93**, 114017 (2016). 327
 288 [10] L. W. Whitlow, *Deep Inelastic Structure Functions From Electron Scattering on Hydrogen, Deuterium, and Iron at $0.6\text{-GeV}^2 \leq Q^2 \leq 30\text{-GeV}^2$* , Ph.D. thesis, Stanford University (1990). 328
 289 [11] L. W. Whitlow *et al.*, *Phys. Lett. B* **282**, 475 (1992). 329
 290 [12] S. P. Malace, *Measurements of Inclusive Resonance Cross Sections for Quark-Hadron Duality Studies*, Ph.D. thesis, Hampton U. (2006). 330
 291 [13] D. Abrams *et al.* (Jefferson Lab Hall A Tritium Collaboration), *Phys. Rev. Lett.* **128**, 132003 (2022). 331
 292 [14] M. Amarian, C. Collaboration, *et al.*, CLAS PROPOSAL PR12-06-113 (2006). 332
 293 [15] N. Baillie *et al.* (CLAS), *Phys. Rev. Lett.* **108**, 142001 (2012), [Erratum: *Phys. Rev. Lett.* **108**, 199902 (2012)], arXiv:1110.2770 [nucl-ex]. 333
 294 [16] K. A. Griffioen *et al.*, *Phys. Rev. C* **92**, 015211 (2015). 334
 295 [17] S. Tkachenko *et al.* (CLAS Collaboration), *Phys. Rev. C* **89**, 045206 (2014). 335
 296 [18] The SHMS 11 GeV/c Spectrometer in Hall C at Jefferson Lab (to be published). 336
 297 [19] D. Bhetuwal, J. Matter, H. Szumila-Vance, C. Ayerbe Gayoso, M. Kabir, D. Dutta, R. Ent, D. Abrams, Z. Ahmed, B. Aljawrneh, *et al.*, *Physical Review C* **108** (2023). 337
 298 [20] D. Bhetuwal *et al.* (The Jefferson Lab Hall C Collaboration), *Phys. Rev. Lett.* **126**, 082301 (2021). 338
 299 [21] L. H. Tao *et al.* (E140X), *Z. Phys. C* **70**, 387 (1996). 339
 300 [22] M. Murphy *et al.* (The Jefferson Lab Hall A Collaboration), *Phys. Rev. C* **100**, 054606 (2019). 340
 301 [23] Y.-S. Tsai, SLAC Preprint SLAC-PUB-848 (1971). 341
 302 [24] L. W. MO and Y. S. TSAI, *Rev. Mod. Phys.* **41**, 205 (1969). 342
 303 [25] A. Sun, Ph.D. thesis, Carnegie Mellon University (2022). 343
 304 [26] F. Araiza Gonzalez, Ph.D. thesis, Stony Brook University (2020). 344
 305 [27] S. Nadeeshani, Ph.D. thesis, Hampton University (2021). 345
 306 [28] D. Biswas, Ph.D. thesis, Hampton University (2022). 346
 307 [29] A. Karki, Ph.D. thesis, Mississippi State University (2022). 347
 308 [30] C. Morean, Ph.D. thesis, University of Tennessee (2023). 348
 309 [31] V. Mamyran, *Measurements of F_2 and $R=\sigma_L/\sigma_T$ on Nuclear Targets in the Nucleon Resonance Region*, Ph.D. thesis (2012), arXiv:1202.1457 [nucl-ex]. 349
 310 [32] S. Dasu, Ph.D. thesis, University of Rochester (1988). 350
 311 [33] N. Sato, C. Andres, J. J. Ethier, and W. Melnitchouk (Jefferson Lab Angular Momentum (JAM) Collaboration), *Phys. Rev. D* **101**, 074020 (2020). 351
 312 [34] E. Moffat, W. Melnitchouk, T. C. Rogers, and N. Sato (Jefferson Lab Angular Momentum (JAM) Collaboration), *Phys. Rev. D* **104**, 016015 (2021). 352
 313 [35] P. E. Bosted and M. E. Christy, *Phys. Rev. C* **77**, 065206 (2008). 353
 314 [36] S. Li, private communication (2022). 354
 315 [37] A. Karki *et al.* (Hall C), *Phys. Rev. C* **108**, 035201 (2023), arXiv:2207.03850 [nucl-ex]. 355
 316 [38] S. Li, A. Accardi, M. Cerutti, I. P. Fernando, C. E. Keppel, W. Melnitchouk, P. Monaghan, G. Niculescu, M. I. Niculescu, and J. F. Owens, *Phys. Rev. D* **109**, 074036 (2024), arXiv:2309.16851 [hep-ph]. 356
 317 [39] D. Abrams *et al.* (Jefferson Lab Hall A Tritium Collaboration), *Phys. Rev. Lett.* **128**, 132003 (2022). 357
 318 [40] C. Cocuzza, C. E. Keppel, H. Liu, W. Melnitchouk, A. Metz, N. Sato, and A. W. Thomas (Jefferson Lab Angular Momentum (JAM) Collaboration), *Phys. Rev. Lett.* **127**, 242001 (2021). 358
 319 [41] R. Acciarri *et al.* (Dune Collaboration), (2016), arXiv:1512.06148. 359